

## Hydrogen Peroxide Adducts

Deutsche Ausgabe: DOI: 10.1002/ange.201606561  
Internationale Ausgabe: DOI: 10.1002/anie.201606561

## Hydrogen Peroxide Coordination to Cobalt(II) Facilitated by Second-Sphere Hydrogen Bonding

Christian M. Wallen, Lukáš Palatinus, John Bacsá, and Christopher C. Scarborough\*

**Abstract:**  $M(\text{H}_2\text{O}_2)$  adducts have been postulated as intermediates in biological and industrial processes; however, only one observable  $M(\text{H}_2\text{O}_2)$  adduct has been reported, where  $M$  is redox-inactive zinc. Herein, direct solution-phase detection of an  $M(\text{H}_2\text{O}_2)$  adduct with a redox-active metal, cobalt(II), is described. This  $\text{Co}^{\text{II}}(\text{H}_2\text{O}_2)$  compound is made observable by incorporating second-sphere hydrogen-bonding interactions between bound  $\text{H}_2\text{O}_2$  and the supporting ligand, a trianionic trisulfonamido ligand. Thermodynamics of  $\text{H}_2\text{O}_2$  binding and decay kinetics of the  $\text{Co}^{\text{II}}(\text{H}_2\text{O}_2)$  species are described, as well as the reaction of this  $\text{Co}^{\text{II}}(\text{H}_2\text{O}_2)$  species with Group 2 cations.

Hydrogen peroxide is an attractive and green industrial oxidant that is readily prepared from  $\text{H}_2$  and  $\text{O}_2$ .<sup>[1,2]</sup> Applications of  $\text{H}_2\text{O}_2$  include bleaching of cotton and wood pulp<sup>[3,4]</sup> and oxygenation of propylene to propylene oxide.<sup>[5]</sup> Oxidations by  $\text{H}_2\text{O}_2$  often employ metal catalysts, possibly involving  $M(\text{H}_2\text{O}_2)$  intermediates, as such adducts have been computationally<sup>[6–9]</sup> and kinetically<sup>[10–13]</sup> implicated. An  $\text{Fe}^{\text{III}}(\text{H}_2\text{O}_2)$  species has been proposed in cytochromes P450 as or en route to the ill-defined “second oxidant”, the key intermediate in a minor oxidation pathway typically overshadowed by the canonical pathway proceeding through Compound I.<sup>[14–17]</sup> A computational study by Shaik et al.<sup>[18]</sup> predicted that longevity of  $\text{Fe}^{\text{III}}(\text{H}_2\text{O}_2)$  adducts in cytochromes P450 is increased when hydrogen-bonding interactions are present between bound  $\text{H}_2\text{O}_2$  and basic moieties in the active-site pocket (**A**, Figure 1). In 2015, we reported the first  $M(\text{H}_2\text{O}_2)$  adduct, a  $\text{Zn}^{\text{II}}$  species (**B**, Figure 1), made observable by incorporating second-sphere hydrogen-bonding interactions between  $\text{H}_2\text{O}_2$  and a trianionic trisulfonamido ancillary ligand.<sup>[19]</sup> Given the presence of a redox-active metal in the putative  $\text{Fe}^{\text{III}}(\text{H}_2\text{O}_2)$  species in cytochromes P450, we became interested in studying the viability of coordination of  $\text{H}_2\text{O}_2$  to redox-active metals. Herein, we detail the first observable  $M(\text{H}_2\text{O}_2)$  adduct bearing a redox-active metal.

The disproportionation of  $\text{H}_2\text{O}_2$  into  $\text{O}_2$  and  $\text{H}_2\text{O}$  is accelerated by redox-active metals,<sup>[1]</sup> so we anticipated that analogues of **B** incorporating redox-active metals would be

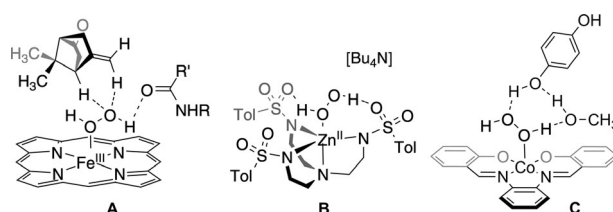
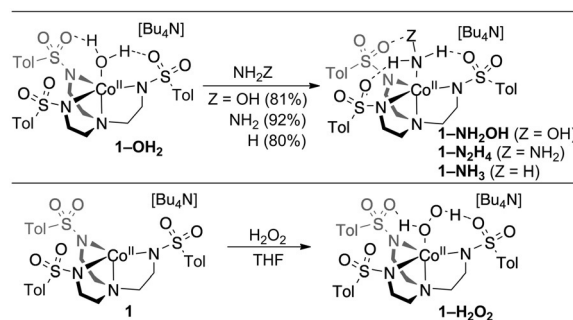


**Figure 1.** Computed structure<sup>[18]</sup> demonstrating the importance of hydrogen bonding in an  $\text{Fe}^{\text{III}}(\text{H}_2\text{O}_2)$  species in cytochromes P450 (**A**); the first  $\text{H}_2\text{O}_2$  coordination compound (**B**);<sup>[19]</sup> and a calculated  $\text{Co}(\text{H}_2\text{O}_2)$  intermediate in aerobic hydroquinone oxidation (**C**).<sup>[9]</sup>

shorter-lived. We chose to explore a  $\text{Co}^{\text{II}}$  analogue of **B**, as a  $\text{Co}^{\text{II}}(\text{H}_2\text{O}_2)$  species (**C**, Figure 1) had recently been computationally implicated as reactive for oxidation of hydroquinone to benzoquinone.<sup>[9]</sup> As described below, our observed  $\text{Co}^{\text{II}}(\text{H}_2\text{O}_2)$  species is shorter-lived than **B**, but its accessibility corroborates the existence of  $M(\text{H}_2\text{O}_2)$  adducts with redox-active metals and provides a platform for developing catalysts for oxidation reactions with  $\text{H}_2\text{O}_2$ .

We initiated our studies with  $[\text{Bu}_4\text{N}][(\text{Ts}_3\text{tren})\text{Co}^{\text{II}}]$  (**1**) and  $[\text{Bu}_4\text{N}][(\text{Ts}_3\text{tren})\text{Co}^{\text{II}}(\text{OH}_2)]$  (**1-OH<sub>2</sub>**)<sup>[20]</sup> (Scheme 1;



**Scheme 1.** Synthesis of **1** and **1-L**. Yields are of crystalline product.

$(\text{Ts}_3\text{tren})^{3-}$  is the ancillary ligand on  $\text{Zn}^{\text{II}}$  in **B**, Figure 1). The  $\text{H}_2\text{O}$  ligand in **1-OH<sub>2</sub>** is readily displaced by  $\text{NH}_2\text{OH}$ ,  $\text{N}_2\text{H}_4$ , or  $\text{NH}_3$  to afford **1-NH<sub>2</sub>OH**, **1-N<sub>2</sub>H<sub>4</sub>**, and **1-NH<sub>3</sub>**, respectively. X-ray crystallographic characterization of these species<sup>[35]</sup> revealed the presence of hydrogen-bonding interactions between the sulfonyl oxygen atoms and the axial-ligand protons (Figure 2), including the protons of the distal heteroatom in  $\text{N}_2\text{H}_4$  and  $\text{NH}_2\text{OH}$ . **1** and **1-OH<sub>2</sub>** are differentiated by electronic absorption spectroscopy,<sup>[20]</sup> however, **1-OH<sub>2</sub>** is not distinguishable from its 5-coordinate nitrogenous analogues **1-NH<sub>2</sub>OH**, **1-N<sub>2</sub>H<sub>4</sub>**, and **1-NH<sub>3</sub>** by this technique

[\*] C. M. Wallen, Dr. J. Bacsá, Prof. Dr. C. C. Scarborough  
Department of Chemistry, Emory University  
1515 Dickey Dr., Atlanta, GA 30322 (USA)  
E-mail: scarborough@emory.edu

Prof. Dr. L. Palatinus  
Department of Structure Analysis  
Institute of Physics of the AS CR, Prague (Czechia)

Supporting information and the ORCID identification number(s) for the author(s) of this article can be found under <http://dx.doi.org/10.1002/anie.201606561>.

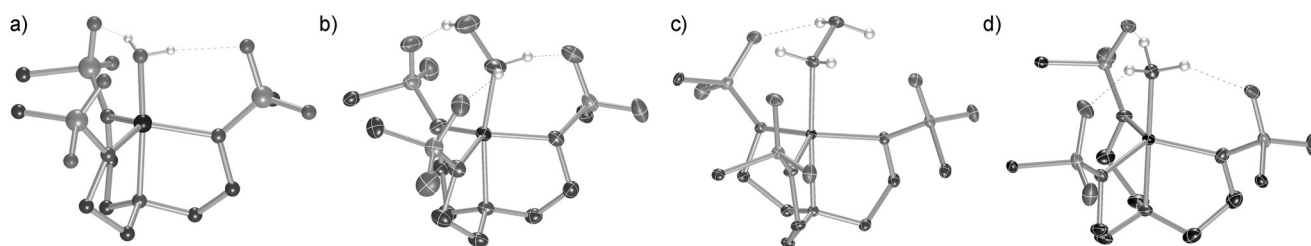


**Figure 2.** Structures of the anions in **1-OH<sub>2</sub>** (a), **1-NH<sub>2</sub>OH** (b), **1-N<sub>2</sub>H<sub>4</sub>** (c), and **1-NH<sub>3</sub>** (d) in the crystalline state, demonstrating intramolecular hydrogen bonding with the axial ligand ([Bu<sub>4</sub>N]<sup>+</sup> ions omitted).<sup>[35]</sup> Tolly groups of the (Ts<sub>3</sub>tren)<sup>3-</sup> ligand are truncated for clarity. Only hydrogen atoms of the axial ligands are shown. **1-OH<sub>2</sub>**, which is very similar to a complex reported by Borovik et al.,<sup>[22]</sup> is an incommensurately modulated structure and is therefore represented as a ball-and-stick model.

except by band intensity, where complexes with axial nitrogen ligands show more intense d-d transitions than **1-OH<sub>2</sub>** (Figure 3).

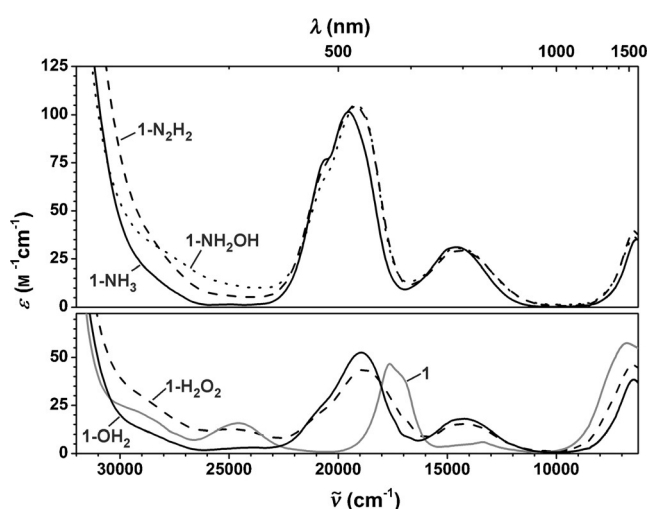


**Figure 3.** Electronic absorption spectra of **1-NH<sub>3</sub>**, **1-N<sub>2</sub>H<sub>4</sub>**, **1-NH<sub>2</sub>OH**, **1-OH<sub>2</sub>**, **1**, and **1-H<sub>2</sub>O<sub>2</sub>**.

In 2015, we reported a method for accessing anhydrous H<sub>2</sub>O<sub>2</sub> in THF.<sup>[19]</sup> Although we have not encountered problems with such solutions, they should be handled with care, as formation of radicals and/or organic peroxides is possible, particularly upon heating or irradiation. Addition of anhydrous H<sub>2</sub>O<sub>2</sub> in THF to **1-OH<sub>2</sub>** did not result in any notable changes in the electronic absorption spectrum, and addition of H<sub>2</sub>O<sub>2</sub> to **1** provided an absorption spectrum of a five-coordinate Co<sup>II</sup> species that was indistinguishable from that of **1-OH<sub>2</sub>** (Figure 3). Despite the redox potential of **1-OH<sub>2</sub>** (+78 mV vs. Fc/Fc<sup>+</sup> in CH<sub>2</sub>Cl<sub>2</sub>),<sup>[20]</sup> no cobalt oxidation products were spectroscopically observable on addition of H<sub>2</sub>O<sub>2</sub> to **1** or **1-OH<sub>2</sub>**.<sup>[21]</sup> Generation of 5-coordinate Co<sup>II</sup> on addition of H<sub>2</sub>O<sub>2</sub> to **1** is consistent with either formation of **1-H<sub>2</sub>O<sub>2</sub>** or formation of **1-OH<sub>2</sub>** as a consequence of immediate H<sub>2</sub>O<sub>2</sub> disproportionation by Co<sup>II</sup>. Distinguishing between these possibilities required a method of directly detecting H<sub>2</sub>O<sub>2</sub> in these **1**/H<sub>2</sub>O<sub>2</sub> solutions. Despite the paramagnetic nature of the complexes studied, <sup>1</sup>H NMR spectroscopy

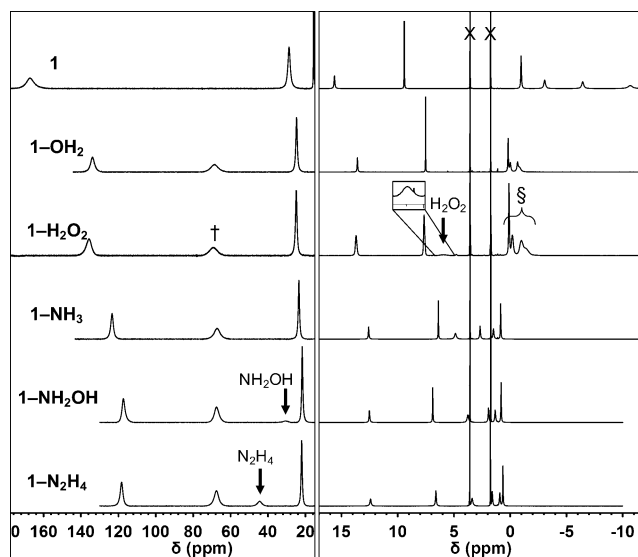


**Figure 4.** <sup>1</sup>H-NMR spectra (in [D<sub>8</sub>]THF) of cobalt complexes scaled to show resonances for visible axial ligands (N<sub>2</sub>H<sub>4</sub>, NH<sub>2</sub>OH, and H<sub>2</sub>O<sub>2</sub>), the presence of alkyl-bridge signals in the 5-coordinate complexes (†), and positions of [Bu<sub>4</sub>N]<sup>+</sup> resonances (§), which are dependent on the number of second-sphere hydrogen bonds (0, 2, or 3). Residual [D<sub>8</sub>]THF signals are indicated by X.

proved a viable technique for studying coordination of H<sub>2</sub>O<sub>2</sub> to **1** (Figure 4).

<sup>1</sup>H NMR resonances associated with **1-L** were assigned by comparing spectra of related complexes (see the Supporting Information). All 5-coordinate Co<sup>II</sup> species showed a CH<sub>2</sub> resonance near 65 ppm, and the presence of this signal in a solution containing H<sub>2</sub>O<sub>2</sub> and **1** (†, Figure 4) corroborates the electronic absorption data (Figure 3) revealing a 5-coordinate Co<sup>II</sup> ion. The positions of the Bu proton resonances of the [Bu<sub>4</sub>N]<sup>+</sup> counterion are affected by the presence of axial ligands on cobalt. In the <sup>1</sup>H NMR spectrum of **1**, the Bu signals are spaced between 1 and –11 ppm, where the large paramagnetic shifting is consistent with interaction between the [Bu<sub>4</sub>N]<sup>+</sup> cation and the cobalt complex in solution, likely through hydrogen bonding between the α-hydrogen atoms on Bu and the sulfonyl oxygen atoms as seen in the solid state. For derivatives **1-L** with three second-sphere hydrogen bonds (**1-NH<sub>2</sub>OH**, **1-NH<sub>3</sub>**, and **1-N<sub>2</sub>H<sub>4</sub>**) the Bu signals are less paramagnetically shifted (0 to 5 ppm), consistent with axial coordination disrupting hydrogen bond-

ing between the ions in solution. For **1-OH<sub>2</sub>**, which only contains two second-sphere hydrogen bonds, the Bu proton resonances overlap between 1 and –1 ppm. When anhydrous H<sub>2</sub>O<sub>2</sub> is combined with **1**, the Bu proton resonances appear between 1 and –2 ppm, similar to **1-OH<sub>2</sub>** (S, Figure 4). These data suggest that the axial ligand in a solution of **1** and anhydrous H<sub>2</sub>O<sub>2</sub> is diprotic, which could be explained by binding of H<sub>2</sub>O or H<sub>2</sub>O<sub>2</sub>. For complexes **1-OH<sub>2</sub>** and **1-NH<sub>3</sub>**, the proton resonances corresponding to the axial ligand are not observable by <sup>1</sup>H NMR spectroscopy, even upon addition of excess ligand (see the Supporting Information). However, <sup>1</sup>H NMR spectra of **1-N<sub>2</sub>H<sub>4</sub>** and **1-NH<sub>2</sub>OH** show signals at 44 ppm and 30 ppm, respectively, corresponding to the axial-ligand protons (Figure 4). The spectrum of a solution of **1** and anhydrous H<sub>2</sub>O<sub>2</sub> contains a broad signal at 5.9 ppm (Figure 4). Over time, this signal shifts to 8.8 ppm (closer to that of free H<sub>2</sub>O<sub>2</sub> at 9.4 ppm) and decreases in intensity following a first-order pathway with a half-life of (353 ± 33) s (Figure 5). This

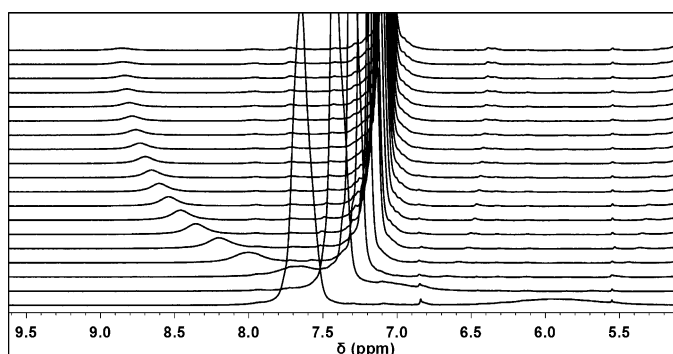


**Figure 5.** Room-temperature decay of **1-H<sub>2</sub>O<sub>2</sub>** measured by <sup>1</sup>H NMR spectroscopy (in [D<sub>8</sub>]THF). The H<sub>2</sub>O<sub>2</sub> resonance shifts from 5.9 ppm to 8.8 ppm. The decay product was confirmed by X-ray crystallography to be **1-OH<sub>2</sub>**.<sup>[35]</sup> The tall signal at 7.7 ppm shifting to 7.1 ppm is a methyl group on the sulfonamidate ligand.

shifted H<sub>2</sub>O<sub>2</sub> resonance is the first direct evidence that H<sub>2</sub>O<sub>2</sub> is binding to Co<sup>II</sup> in **1**, as the <sup>1</sup>H NMR and electronic spectra demonstrate that Co<sup>II</sup> is five-coordinate under these conditions. The decay product of **1-H<sub>2</sub>O<sub>2</sub>** was identified as **1-OH<sub>2</sub>** by crystallization of the bulk material. The shifting H<sub>2</sub>O<sub>2</sub> resonance throughout decay of **1-H<sub>2</sub>O<sub>2</sub>** points to an equilibrium between free and bound H<sub>2</sub>O<sub>2</sub> that is perturbed by H<sub>2</sub>O formed upon H<sub>2</sub>O<sub>2</sub> disproportionation, leading us to examine the equilibrium constants of binding H<sub>2</sub>O<sub>2</sub> and H<sub>2</sub>O to **1**.

To probe whether H<sub>2</sub>O<sub>2</sub> binding is perturbed by the presence of H<sub>2</sub>O, H<sub>2</sub>O<sub>2</sub> was added to **1-OH<sub>2</sub>** and its decay monitored by <sup>1</sup>H NMR spectroscopy. Initially, the H<sub>2</sub>O<sub>2</sub> resonance appeared at 8.8 ppm (c.f. 5.9 ppm in the absence of H<sub>2</sub>O) and then shifted toward 9.1 ppm [*t*<sub>1/2</sub> = (1190 ± 10) s]. When H<sub>2</sub>O<sub>2</sub> was added to **1-NH<sub>3</sub>**, the H<sub>2</sub>O<sub>2</sub> resonance remained at 9.5 ppm and decayed with a half-life of (13700 ± 200) s. These data are consistent with H<sub>2</sub>O<sub>2</sub> disproportionation occurring upon coordination to **1**, and with H<sub>2</sub>O<sub>2</sub> being a weaker ligand for **1** than H<sub>2</sub>O or NH<sub>3</sub>, consistent with descriptions of H<sub>2</sub>O<sub>2</sub> as a very poor ligand.<sup>[23–27]</sup> The first-order decay of **1-H<sub>2</sub>O<sub>2</sub>** contrasts the second-order decay mechanism

of **B**, which bears the same ligand and counterion, and at the same starting concentration has a half-life of 10<sup>4</sup> s.<sup>[19]</sup> This comparison suggests that the redox-active nature of M has a dramatic effect on the stability of M(H<sub>2</sub>O<sub>2</sub>) species.

We sought to quantify binding affinities of **1** for H<sub>2</sub>O and H<sub>2</sub>O<sub>2</sub>. H<sub>2</sub>O<sub>2</sub> has been described as a poor ligand<sup>[23–27]</sup> such that its coordination to metals was not unambiguously detected until 2015.<sup>[19]</sup> Prikhodchenko et al. demonstrated that H<sub>2</sub>O<sub>2</sub> is a more effective hydrogen-bond donor than H<sub>2</sub>O, clarifying the importance of second-sphere hydrogen bonding in H<sub>2</sub>O<sub>2</sub> coordination.<sup>[27–30]</sup> Because of the short lifetime of **1-H<sub>2</sub>O<sub>2</sub>**, we turned to photometric titrations using electronic absorption spectroscopy to determine the binding constants for H<sub>2</sub>O and H<sub>2</sub>O<sub>2</sub> to **1** at –70 °C, as decay of **1-H<sub>2</sub>O<sub>2</sub>** cannot be detected within one hour at temperatures below –40 °C by NMR spectroscopy. Titration of **1** with H<sub>2</sub>O or anhydrous H<sub>2</sub>O<sub>2</sub> in THF at –70 °C afforded the curves shown in Figure 6, from which *K*<sub>eq</sub> values for the coordination of H<sub>2</sub>O<sub>2</sub> and H<sub>2</sub>O to **1** are derived: (31.3 ± 0.2) M<sup>–1</sup> and (31 600 ± 12 600) M<sup>–1</sup> at –70 °C, respectively. These data establish a preference for binding of **1** to H<sub>2</sub>O over H<sub>2</sub>O<sub>2</sub>, where *K*<sub>eq</sub> for displacing H<sub>2</sub>O<sub>2</sub> in **1-H<sub>2</sub>O<sub>2</sub>** by H<sub>2</sub>O at –70 °C is (1010 ± 400) (Δ*G* = –2.8 kcal mol<sup>–1</sup>). To our knowledge, this is the first H<sub>2</sub>O<sub>2</sub>/metal binding constant measured.

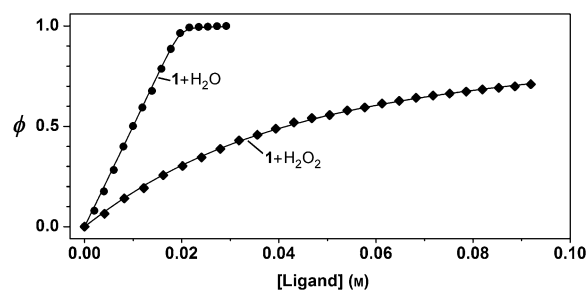
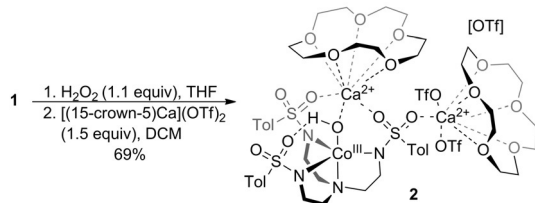


**Figure 6.** Photometric titrations of **1** with H<sub>2</sub>O and H<sub>2</sub>O<sub>2</sub> in THF at –70 °C. Data are plotted as fractional saturation vs. concentration of the ligand (H<sub>2</sub>O or H<sub>2</sub>O<sub>2</sub>). The curves, which are nonlinear fits to the data, enable calculation of *K*<sub>eq</sub> [(3.16 ± 1.26) × 10<sup>4</sup> M<sup>–1</sup> for H<sub>2</sub>O and (31.3 ± 0.2) M<sup>–1</sup> for H<sub>2</sub>O<sub>2</sub>].

Finally, we probed the reactivity of **1-H<sub>2</sub>O<sub>2</sub>**. Borovik et al. reported that a species closely related to **1** is inert to PhIO, but upon addition of Group 2 ions, oxidation of the Co<sup>II</sup> center by PhIO afforded an isolable Co<sup>III</sup>(μ-OH)Ca<sup>2+</sup> species.<sup>[22]</sup> This transformation may involve a transient Co<sup>IV</sup> intermediate, as redox-inert cations are known to facilitate two-electron oxidation of Co<sup>II</sup> to Co<sup>IV</sup>.<sup>[31,32]</sup> We probed whether Group 2 ions could similarly promote cobalt oxidation and cleavage of the O–O bond of H<sub>2</sub>O<sub>2</sub> in **1-H<sub>2</sub>O<sub>2</sub>**. We have shown that **1** and related species react readily with Group 2 ions to afford heterotrimetallic sandwich compounds.<sup>[20]</sup> Addition of M(OTf)<sub>2</sub> (M = Ca<sup>2+</sup>, Sr<sup>2+</sup>, or Ba<sup>2+</sup>) to **1-H<sub>2</sub>O<sub>2</sub>** resulted in rapid conversion into intensely green products, each with nearly identical electronic absorption spectra. The spectroscopic properties of these green species did not satisfactorily agree with Borovik's report of a red-brown Co<sup>III</sup>(μ-OH)Ca<sup>2+</sup> species;<sup>[22]</sup> however, combination of [(15-crown-5)Ca](OTf)<sub>2</sub>

and **1-H<sub>2</sub>O<sub>2</sub>** afforded X-ray-quality crystals of a Co<sup>III</sup>(μ-OH)Ca<sup>2+</sup> complex (**2**, Scheme 2),<sup>[35]</sup> demonstrating Group 2 ion induced oxidation of Co<sup>II</sup> to Co<sup>III</sup> by H<sub>2</sub>O<sub>2</sub>. The oxidation potential of **1-OH<sub>2</sub>** is +78 mV vs. Fc/Fc<sup>+</sup> in CH<sub>2</sub>Cl<sub>2</sub>,<sup>[20]</sup> so the oxidative stability of the Co<sup>II</sup> ion in **1-H<sub>2</sub>O<sub>2</sub>** suggests that one-electron redox processes involving **1-H<sub>2</sub>O<sub>2</sub>** are not preferred.



**Scheme 2.** Reaction of **1-H<sub>2</sub>O<sub>2</sub>** with Ca<sup>2+</sup> to form **2**. The crystal structure analysis of **2** is included in the Supporting Information. DCM: dichloromethane.

We expect that the Group 2 ions are brought into close proximity with coordinated H<sub>2</sub>O<sub>2</sub> in **1-H<sub>2</sub>O<sub>2</sub>**, as we<sup>[20]</sup> and Borovik et al.<sup>[22,33]</sup> have shown that such sulfonyl oxygen atoms bind Group 2 metal ions without significantly impacting the electronic properties of Co<sup>II</sup>. We hypothesize that the Group 2 ion induced oxidative conversion of **1-H<sub>2</sub>O<sub>2</sub>** into **2** may involve a transient Co<sup>IV</sup>(oxo)/Ca<sup>2+</sup>(OH<sub>2</sub>) or Co<sup>IV</sup>(OH)/Ca<sup>2+</sup>(OH) species that rapidly reacts with a hydrogen-atom donor, likely THF, to afford the observed Co<sup>III</sup> species **2**. Rapid decomposition of Co<sup>IV</sup> has been demonstrated in the instability of related Co<sup>IV</sup>(oxo)<sup>[22,31,32]</sup> and Co<sup>IV</sup>(nitrido)<sup>[34]</sup> species. Regardless of mechanism, the Group 2 ion induced conversion of **1-H<sub>2</sub>O<sub>2</sub>** into **2** provides a new approach to H<sub>2</sub>O<sub>2</sub> activation involving coordination to one metal center and activation by a second metal center. We are currently exploring this dual activation of H<sub>2</sub>O<sub>2</sub> for use in oxidation catalysis.

In summary, we have obtained the first direct evidence for formation of an M(H<sub>2</sub>O<sub>2</sub>) complex with a redox-active metal. Mixing **1** and anhydrous H<sub>2</sub>O<sub>2</sub> resulted in coordination of an axial ligand to cobalt(II) at temperatures where H<sub>2</sub>O<sub>2</sub> is not disproportionated by **1**, and low-temperature photometric titration of **1** with H<sub>2</sub>O<sub>2</sub> or H<sub>2</sub>O, as well as decay kinetics of **1-H<sub>2</sub>O<sub>2</sub>** in the presence of H<sub>2</sub>O, revealed that H<sub>2</sub>O<sub>2</sub> is a weaker ligand for the Co<sup>II</sup> center in **1** than H<sub>2</sub>O. **1-H<sub>2</sub>O<sub>2</sub>** is stable to oxidation of the Co<sup>II</sup> center, but addition of [(15-crown-5)Ca](OTf)<sub>2</sub> induced oxidation to afford the Co<sup>III</sup>(μ-OH)Ca<sup>2+</sup> complex **2**. Activation of coordinated H<sub>2</sub>O<sub>2</sub> by a secondary metal is a novel approach to developing oxidation reactions with H<sub>2</sub>O<sub>2</sub>, and our efforts on expanding the coordination chemistry of H<sub>2</sub>O<sub>2</sub> and exploiting the reactivity of M(H<sub>2</sub>O<sub>2</sub>) adducts are on-going.

## Acknowledgements

This work was enabled by funds from a National Science Foundation CAREER award (CHE-1455211).

**Keywords:** cobalt · hydrogen bonds · peroxides · peroxido ligands · second-sphere interactions

**How to cite:** *Angew. Chem. Int. Ed.* **2016**, *55*, 11902–11906  
*Angew. Chem.* **2016**, *128*, 12081–12085

- [1] C. W. Jones, *Applications of Hydrogen Peroxide and Derivatives*, Royal Society, Cambridge, UK, **1999**.
- [2] M. Lancaster, *Green Chemistry*, Royal Society, Cambridge, UK, **2002**.
- [3] R. Hage, J. W. de Boer, F. Gaulard, K. Maaijen, *Adv. Inorg. Chem.* **2013**, *65*, 85–116.
- [4] R. Hage, A. Lienke, *Angew. Chem. Int. Ed.* **2006**, *45*, 206–222; *Angew. Chem.* **2006**, *118*, 212–229.
- [5] V. Russo, R. Tesser, E. Santacesaria, M. Di Serio, *Ind. Eng. Chem. Res.* **2013**, *52*, 1168–1178.
- [6] M. Chen, Y. Pan, H.-K. Kwong, R. J. Zeng, K.-C. Lau, T.-C. Lau, *Chem. Commun.* **2015**, *51*, 13686–13689.
- [7] H.-K. Kwong, P.-K. Lo, K.-C. Lau, T.-C. Lau, *Chem. Commun.* **2011**, *47*, 4273–4275.
- [8] L. Ma, Y. Pan, W.-L. Man, H.-K. Kwong, W. W. Y. Lam, G. Chen, K.-C. Lau, T.-C. Lau, *J. Am. Chem. Soc.* **2014**, *136*, 7680–7687.
- [9] C. W. Anson, S. Ghosh, S. Hammes-Schiffer, S. S. Stahl, *J. Am. Chem. Soc.* **2016**, *138*, 4186–4193.
- [10] P. Afanasiev, E. V. Kudrik, J.-M. M. Millet, D. Bouchu, A. B. Sorokin, *Dalton Trans.* **2011**, *40*, 701–710.
- [11] S. A. Mirza, B. Bocquet, C. Robyr, S. Thomi, A. F. Williams, *Inorg. Chem.* **1996**, *35*, 1332–1337.
- [12] A. Theodoridis, J. Maigut, R. Puchta, E. V. Kudrik, R. van Eldik, *Inorg. Chem.* **2008**, *47*, 2994–3013.
- [13] M. Wolak, R. van Eldik, *Chem. Eur. J.* **2007**, *13*, 4873–4883.
- [14] M. J. Coon, *Annu. Rev. Pharmacol. Toxicol.* **2005**, *45*, 1–25.
- [15] I. G. Denisov, T. M. Makris, S. G. Sligar, I. Schlichting, *Chem. Rev.* **2005**, *105*, 2253–2278.
- [16] *Cytochrome P450: Structure, Mechanism, and Biochemistry* (Ed.: P. R. Ortiz de Montellano), Kluwer Academic/Plenum Publishers, New York, **2005**.
- [17] S. Shaik, D. Kumar, S. P. de Visser, A. Altun, W. Thiel, *Chem. Rev.* **2005**, *105*, 2279–2328.
- [18] B. Wang, C. Li, K. D. Dubey, S. Shaik, *J. Am. Chem. Soc.* **2015**, *137*, 7379–7390.
- [19] C. M. Wallen, J. Bacsá, C. C. Scarborough, *J. Am. Chem. Soc.* **2015**, *137*, 14606–14609.
- [20] C. M. Wallen, M. Wieliczko, J. Bacsá, C. C. Scarborough, *Inorg. Chem. Front.* **2016**, *3*, 142–149.
- [21] Since related Co<sup>III</sup> species display intense electronic transitions in the visible region,<sup>[31]</sup> the presence of >0.1% Co<sup>III</sup> would be visible by electronic absorption spectroscopy in solutions of **1** and H<sub>2</sub>O<sub>2</sub>.
- [22] D. C. Lacy, Y. J. Park, J. W. Ziller, J. Yano, A. S. Borovik, *J. Am. Chem. Soc.* **2012**, *134*, 17526–17535.
- [23] A. G. DiPasquale, J. M. Mayer, *J. Am. Chem. Soc.* **2008**, *130*, 1812–1813.
- [24] A. G. Medvedev, A. A. Mikhaylov, A. V. Churakov, M. V. Vener, T. A. Tripol'skaya, S. Cohen, O. Lev, P. V. Prikhodchenko, *Inorg. Chem.* **2015**, *54*, 8058–8065.
- [25] A. A. Mikhaylov, A. G. Medvedev, A. V. Churakov, D. A. Grishanov, P. V. Prikhodchenko, O. Lev, *Chem. Eur. J.* **2016**, *22*, 2980–2986.
- [26] A. V. Churakov, S. Sladkevich, O. Lev, T. A. Tripol'skaya, P. V. Prikhodchenko, *Inorg. Chem.* **2010**, *49*, 4762–4764.
- [27] Y. Wolanov, A. Shurki, P. V. Prikhodchenko, T. A. Tripol'skaya, V. M. Novotortsev, R. Pedahzur, O. Lev, *Dalton Trans.* **2014**, *43*, 16614–16625.
- [28] A. V. Churakov, P. V. Prikhodchenko, J. A. K. Howard, O. Lev, *Chem. Commun.* **2009**, 4224–4226.



- [29] P. V. Prihodchenko, A. G. Medvedev, T. A. Tripol'skaya, A. V. Churakov, Y. Wolanov, J. A. K. Howard, O. Lev, *CrystEngComm* **2011**, *13*, 2399–2407.
- [30] M. V. Vener, A. G. Medvedev, A. V. Churakov, P. V. Prihodchenko, T. A. Tripol'skaya, O. Lev, *J. Phys. Chem. A* **2011**, *115*, 13657–13663.
- [31] S. Hong, F. F. Pfaff, E. Kwon, Y. Wang, M.-S. Seo, E. Bill, K. Ray, W. Nam, *Angew. Chem. Int. Ed.* **2014**, *53*, 10403–10407; *Angew. Chem.* **2014**, *126*, 10571–10575.
- [32] F. F. Pfaff, S. Kundu, M. Risch, S. Pandian, F. Heims, I. Pryjomska-Ray, P. Haack, R. Metzinger, E. Bill, H. Dau, P. Comba, K. Ray, *Angew. Chem. Int. Ed.* **2011**, *50*, 1711–1715; *Angew. Chem.* **2011**, *123*, 1749–1753.
- [33] S. A. Cook, A. S. Borovik, *Acc. Chem. Res.* **2015**, *48*, 2407–2414.
- [34] E. M. Zolnhofer, M. KäB, M. M. Khusniyarov, F. W. Heinemann, L. Maron, M. van Gastel, E. Bill, K. Meyer, *J. Am. Chem. Soc.* **2014**, *136*, 15072–15078.
- [35] CCDC 144760 (**1-OH<sub>2</sub>**), 144761 (**1-N<sub>2</sub>H<sub>4</sub>**), 144762 (**1-NH<sub>2</sub>OH**), 144763 (**2**), and 1489712 (**1-NH<sub>3</sub>**) contain the supplementary crystallographic data for this paper. These data can be obtained free of charge from The Cambridge Crystallographic Data Centre.

Received: July 6, 2016

Published online: August 25, 2016